Temperature effects on the 15–85 μm spectra of olivines and pyroxenes

J. E. Bowey,[1,2]★ C. Lee,[1] C. Tucker,[1] A. M. Hofmeister,[3] P. A. R. Ade[1] and M. J. Barlow[2]

[1]*Department of Physics, Queen Mary, University of London, Mile End Road, London E1 4NS*
[2]*Department of Physics & Astronomy, University College London, Gower Street, London WC1E 6BT*
[3]*Department of Earth & Planetary Science, Washington University, 1 Brookings Drive, St Louis, MO 63110, USA*

ABSTRACT

Far-infrared spectra of laboratory silicates are normally obtained at room temperature even though the grains responsible for astronomical silicate emission bands seen at wavelengths $>20\,\mu m$ are likely to be at temperatures below $\sim 150\,K$. In order to investigate the effect of temperature on silicate spectra, we have obtained absorption spectra of powdered forsterite and olivine, along with two orthoenstatites and diopside clinopyroxene, at $3.5 \pm 0.5\,K$ and at room temperature ($295 \pm 2\,K$). To determine the changes in the spectra the resolution must be increased from ~ 1 to $0.25\,cm^{-1}$ at both temperatures, because a reduction in temperature reduces the phonon density, thereby reducing the width of the infrared peaks. Several bands observed at 295 K split at 3.5 K. At 3.5 K the widths of isolated single bands in olivine, enstatites and diopside are ~ 90 per cent of their 295-K widths. However, in forsterite the 3.5-K widths of the 31-, 49- and 69-μm bands are, respectively, 90, 45 and 31 per cent of their 295-K widths. Owing to an increase in phonon energy as the lattice contracts, 3.5-K singlet peaks occur at shorter wavelengths than do the corresponding 295-K peaks; the magnitude of the wavelength shift increases from ~ 0–$0.2\,\mu m$ at 25 μm to $\sim 0.9\,\mu m$ at 80 μm. In olivines and enstatites the wavelength shifts can be approximated by polynomials of the form $ax + bx^2$ where $x = \lambda_{pk}(295\,K)$ and the coefficients a and b differ between minerals; for diopside this formula gives a lower limit to the shift. Changes in the relative absorbances of spectral peaks are also observed. The temperature dependence of λ_{pk} and bandwidth shows promise as a means to deduce characteristic temperatures of mineralogically distinct grain populations. In addition, the observed changes in band strength with temperature will affect estimates of grain masses and relative mineral abundances inferred using room-temperature laboratory data. Spectral measurements of a variety of minerals at a range of temperatures are required to quantify these effects fully.

Key words: line: identification – techniques: spectroscopic – stars: circumstellar matter – dust, extinction – ISM: lines and bands – infrared: general.

1 INTRODUCTION

Mid- and far-infrared spectra obtained with the *Infrared Space Observatory* (*ISO*) Short- and Long-Wavelength Spectrometers (SWS and LWS, respectively) have revealed emission bands which have been associated with crystalline silicate dust. The environments include comets, young stellar objects and oxygen-rich dust in outflows and discs associated with late-type stars and planetary nebulae (e.g. Waters et al. 1996; Cohen et al. 1999; Malfait et al. 1999; Sylvester et al. 1999; Crovisier et al. 2000; respectively). Simple spectral fits indicate that much of the optically thin silicate emission occurs at temperatures in the

50–100 K range (e.g. Sylvester et al. 1999). However, previous laboratory studies (e.g. Day 1976; Agladze et al. 1996; Henning & Mutschke 1997; Mennella et al. 1998) have shown that the optical properties of silicates vary between 295 and 10 K. In MgO the frequency and FWHM(ν) of the 24.5-μm (295-K) TO mode (Jasperse et al. 1964) vary nearly linearly with temperature between 7.5 and 1950 K (Kachare, Andermann & Brantley 1972). A similar study of the effect of 423–873 K temperatures on 3–12 μm PAH bands by Joblin et al. (1995) revealed changes in band structure, bandwidth and frequency which indicate that free (as opposed to condensed) PAH molecules carry the astronomical 3.3-μm band.

Owing to a lack of laboratory data, both simple blackbody fits and radiative transfer models of these environments have used

★E-mail: jeb@star.ucl.ac.uk

silicate laboratory spectra obtained at room temperature. In addition to fitting *ISO* data, spectra obtained for a range of samples and temperatures will also be required for comparison with data from the Space Infrared Telescope Facility (SIRTF), the Herschel Telescope and the Next Generation Space Telescope (NGST). To begin to quantify the effect of temperature on silicates we compare spectra of two olivines, two orthoenstatites and diopside clinopyroxene at 295 and 3.5 K.

1.1 Choice of spectral resolution

At cryogenic temperatures the vibrational states of a solid are substantially depopulated in comparison with their values at 295 K in accord with statistical thermodynamics. From the damped harmonic oscillator model, the width of a peak is related to the lifetime between phonon scattering events (Wooten 1972; Hofmeister 1999). As the number of states decreases, the possibilities of scattering decrease, and the peaks must therefore sharpen. The vibrational bands observed in cryogenic 10–100 μm spectra of *crystalline* silicates (Day 1976; Henning & Mutschke 1997) are sharper and deeper than those obtained at room temperature. Medium (~1–2 cm^{-1}) resolution spectra (Henning & Mutschke 1997; Mutschke, private communication; Mennella et al. 1998) indicate that the bands of crystalline silicates shift in wavelength as the temperature is reduced, and that the magnitude of the shift increases with wavelength. If the spectral resolution is insufficient, very narrow peaks are undersampled, leading to rounded profiles and incorrect measurements of the wavelength shifts. Therefore, higher resolution measurements are crucial in the far-IR where lower resolution data (Mennella et al. 1998) showed that the isolated ~70-μm (143 cm^{-1}) peak of forsterite has a 24-K width of ~4 cm^{-1} and a ~2 cm^{-1} shift between 295 and 24 K. We therefore present 0.25 cm^{-1} resolution transmission spectra of crystalline minerals from the olivine and pyroxene groups at 3.5 and 295 K.

2 LATTICE STRUCTURES AND 295-K BAND ASSIGNMENTS

2.1 Olivines

The general formula for the olivine solid solution series is $(Mg_xFe_{1-x})_2SiO_4$; the Mg^{2+} end-member is forsterite, the Fe^{2+} end member is fayalite. Olivine minerals have the structure shown in Fig. 1. In the figure each tetrahedron represents the SiO_4^{4-} anion, which consists of an Si atom surrounded by oxygen atoms at each corner of the tetrahedron; M1 and M2 represent the sites of the metal cations. In end-member forsterite both sites are occupied by Mg^{2+}. In olivine some of the Mg^{2+} in sites M1 and M2 is replaced by Fe^{2+}; in this case there is no preference for substitution between the sites since these two ions have similar radii. The active modes in the 15–85 μm region are (after Hofmeister 1997) bending of the tetrahedral O–Si–O [λ(295 K) ≲ 20 μm], rotation of the SiO_4^{4-} tetrahedra (four bands between 21 and 26 μm), translation of the SiO_4^{4-} tetrahedra (~50 μm) and translation of the Mg^{2+} and Fe^{2+} cations (several of the bands in the 21–30 μm region); two bands are associated with combined translations of the divalent cations and SiO_4^{4-} tetrahedra (at ~36.5 and ~70 μm in forsterite; at ~94 and ~109 μm in fayalite, Fe_2SiO_4).
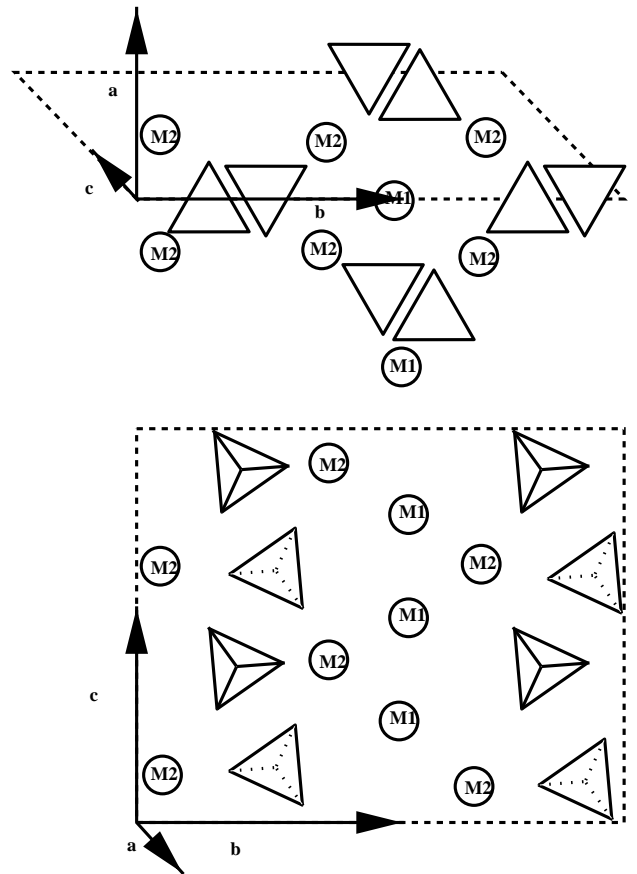
Figure 1. Schematic three-dimensional structure of crystalline olivines. The lower diagram is a slice through the upper diagram along the *b* axis. Tetrahedra represent SiO_4^{4-} groups, the apexes of which point out of the page (solid) and into the page (dotted). M1 and M2 represent the sites of divalent metal cations.
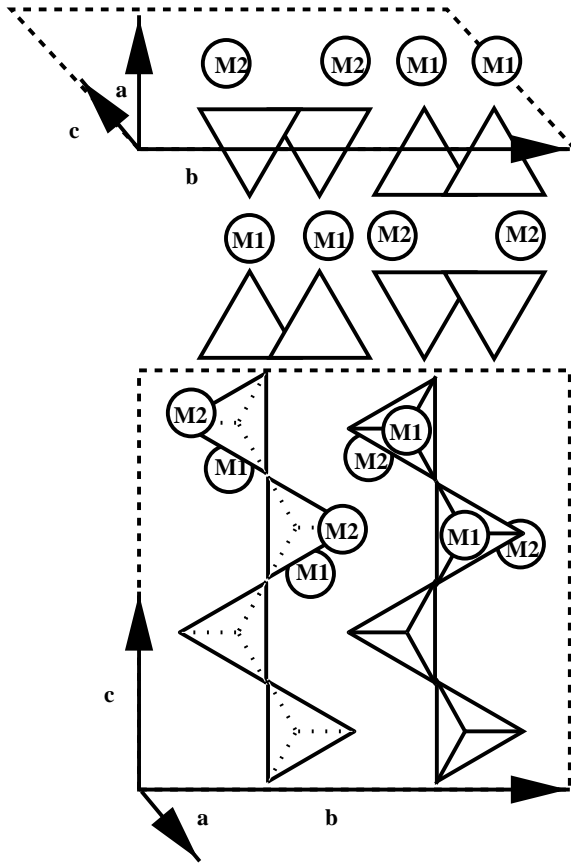
2.2 Ortho- and clino-pyroxenes

Minerals in the pyroxene solid solution series $(Mg_x, Fe_y, Ca_z)_2Si_2O_6$, where $x + y + z = 1$, belong to one of two crystal systems: orthorhombic, in which the three crystal axes are orthogonal, and monoclinic, which has two orthogonal and one inclined axis. The structure of orthopyroxene is shown in Fig. 2; silicate tetrahedra are joined together by shared oxygen atoms to form long chains along the *c* axis. Once again, Mg^{2+} and Fe^{2+} can replace each other in the M1 and M2 sites. The precise band assignments for the orthopyroxenes are unknown. However, comparison with the bands of the clinopyroxenes and olivines suggests that the bands longwards of 20 μm may involve translations of the cations, whereas bands at wavelengths shorter than 20 μm involve the deformation of the tetrahedral and inter-tetrahedral O–Si–O bonds.

In clinopyroxenes similar to diopside (there are other types of clinopyroxene), the larger Ca^{2+} ion (r ~ 1.12 Å) occurs only in the M2 sites, whilst the smaller Mg^{2+} (r ~ 0.72 Å) and Fe^{2+} (r ~ 0.78 Å) ions occur in both these and the smaller M1 sites. This changes the alignment of the tetrahedra, resulting in a crystal shape with an inclined *a* axis. Band assignments in diopsides are currently derived by comparison between force-constant calculations and laboratory data. The active modes in the 15–85 μm region are modelled as follows (Tomisaka & Iishi 1980): bending

of the tetrahedral and inter-tetrahedral O–Si–O bonds shortwards of 30 μm at 295 K (at 23.2 and 29.6 μm these may be blended with Mg^{2+} translations); Mg^{2+} translations blended with translations of the O–Si–O chain and rotations of the tetrahedra at 32.3 μm; Mg^{2+} translations blended with tetrahedral rotations at 34.3 μm; Ca^{2+} translations blended with tetrahedral rotations at 40.4 μm; Ca^{2+} translations at 44.9 μm; finally a broad band at $\sim$66 μm is produced by a zig-zag motion of bridging oxygen atoms in the silicate chain. However, force-constant models are not backed up by laboratory measurements, and the assignments are tentative. Measurements of the effect of isotopic or chemical substitutions are needed for reliable band assignments.

3 THE EFFECT OF TEMPERATURE

3.1 Changes in bond length

If the bond length decreases, the energy of the associated phonon increases. (This physics is equivalent to the energy levels of a particle in a box; the effect is frequently observed in pressure studies, e.g. Ferraro 1984.) Frequency increases as pressure increases (or temperature decreases), and therefore the wavelength of the infrared peak must decrease. Tetrahedral Si–O bond lengths and bond angles are relatively incompressible in comparison with the spacings between the oxygen and metal ions and inter-tetrahedral oxygen atoms, so there is little variation in the wavelength of the 10-μm stretching and 20-μm bending features with temperature (e.g. Day 1976). In contrast, the volumes of the divalent-cation sites are more compressible. Therefore one would expect to see a greater change in the wavelengths of peaks associated with the cation sites.

3.2 Changes in band occupancy

The lifetime, Γ, of a phonon (the time between scattering events) is given by $\Gamma^{-1} \propto 2\pi\Delta\nu(\epsilon_2)$, where $\Delta\nu(\epsilon_2)$ is the full width at half-maximum (FWHM) of the peak in the imaginary part of the dielectric function, ϵ_2, in frequency units (Wooten 1972). When the bands are narrow and weak, the frequency for the atoms vibrating parallel to the propagation direction of the radiation (the longitudinal optic; LO) is similar to the frequency of the atoms vibrating perpendicular to the propagation direction (the transverse optic; TO), thereby creating a symmetrical absorption peak, the shape of which approaches the Lorentzian shape of its counterpart in ϵ_2 (Hofmeister & Mao 2001). Absorbance FWHMs are related to dielectric widths; therefore the widths of the absorbance peaks should be roughly proportional to the dielectric widths in wavenumbers.

At temperature, T, the occupation of phonon energy levels relative to the ground state is given by the partition function $q = \sum_{n=0}^{\infty} \exp[-(nh\nu)/(kT)]$, where k is the Boltzmann constant

Figure 2. Schematic three-dimensional structure of ortho-enstatite. The lower diagram is a slice through the upper diagram along the *b* axis. The *b*–*c* plane is characterized by chains of silicate tetrahedra joined by shared oxygen atoms. These are surrounded by metal ions (for clarity these are omitted from the lower pairs of tetrahedra in each chain). In the *a*–*b* plane M1 and M2 sites occur, respectively, at the apexes and bases of the silicate tetrahedra. M2 sites are larger than M1 sites; therefore in diopside-like clinopyroxenes relatively large Ca^{2+} ions can occupy M2 sites but only smaller Mg^{2+} and Fe^{2+} ions may occupy the M1 sites.

Table 1. Origin and composition of crystalline samples.

Group	Mineral	Composition	Source
Olivine	Synthetic Forsterite[a]	Mg_2SiO_4	Geophysical Laboratory, Washington, D. C., USA.
	Olivine (var. peridot)	$(Mg_{1.77}Fe_{0.20}Al_{0.01}Ni_{0.01})SiO_4$	Navajo IndianReservation San Carlos, Arizona, USA
Orthopyroxene	Enstatite	$(Mg_{1.8}Fe_{0.16}Ca_{0.02})(Si_{1.88}Al_{0.12})O_6$	Fiskenaesset, Greenland
	Bramble Enstatite	$(Mg_{1.7}Fe_{0.28}Ca_{0.01})Si_2O_6$	Bramble, Norway
Clinopyroxene	Diopside	$(Ca_{0.992}Na_{0.028}Mg_{0.94}Fe^{2+}_{0.017}Fe^{3+}_{0.013}Cr_{0.002}Al_{0.015})Si_2O_6$	Dekalb,NY, USA Smithsonian sample R18682

[a]Synthesized from oxide powders by H. K. Mao. X-ray diffraction study analysis by G. Cressey revealed Mg_2SiO_4 forsterite crystals plus $\lesssim$1 per cent by mass of clinopyroxene ($MgSiO_3$) crystals and quartz (SiO_2) crystals which were not detected in any infrared spectra. The grains are coated with $\sim$10 Å of Pt metal from the preparation apparatus.

and it is assumed that the phonon frequency, ν, is not a function of temperature (this is not true; see Section 3.1). As the temperature is decreased the number of vibrational states decreases and the numbers of phonon–phonon scattering events decrease so that phonon scattering off the crystal sides and defects becomes more important. For phonon–phonon scattering, the lifetime is inversely proportional to the number of phonons available, and hence as the sample is cooled, states are depopulated, and the lifetime increases and peak width decreases. In practise, FWHMs are not often measured and the FWHM temperature dependence is not well understood (see Hofmeister, in preparation).

4   THE EXPERIMENT

4.1   Sample preparation

Bulk samples of the minerals listed in Table 1 were broken into smaller pieces with a hammer and then ground to powders by hand with a ceramic pestle and mortar. Grain size was measured by visual inspection in a binocular microscope at ×63 magnification. Small quantities of powder were mixed with petroleum jelly on 0.8-mm-thick polyethylene substrates. Preliminary room temperature measurements at Washington University indicated that the grain sizes and the numbers of grains on each substrate were sufficient to resolve most infrared bands. At Queen Mary, University of London (QMUL), the samples and substrates were cut down and placed in brass holders. The 295- and 3.5-K measurements for each mineral were performed with a single sample and the same spectrometer. The only difference between the measurements was the positioning of the sample in the instrument beam and the temperature of the sample. Hence, the substrate, the coverage of the substrate and the column density were *identical* for each measurement of a specimen.

4.2   Cryogenics and spectroscopy

Spectra were obtained at QMUL using a Martin–Puplett polarizing Fourier Transform Spectrometer with a mercury arc lamp source and a liquid-helium-cooled bolometer pumped to 1.5 K. For the room temperature (295 K) measurements, the sample was placed in the output beam of the spectrometer; the 3.5-K tests were performed by putting the samples in a filter wheel in front of the detector within the 1.5-K bath in the cryostat. As the sample was heated by incident radiation from the arc lamp, it was slightly warmer than the bath, at 3.5 ± 0.5 K. The spectral resolution was selected by inspection of the interferogram; to resolve the fine structure of end-member forsterite at 3.5 K the resolution must be increased to $0.25 \, \text{cm}^{-1}$, whilst a resolution of $2 \, \text{cm}^{-1}$ is adequate at 295 K. For consistency, all spectra at all temperatures were obtained at the higher resolution of $0.25 \, \text{cm}^{-1}$.

For each temperature, reference spectra of the open aperture and petroleum jelly on a polyethylene slide were obtained and then divided into the spectrum of the sample to remove instrumental and substrate effects. For the 3.5-K transmittance spectra, there is an uncertainty in the flux calibration. Therefore the 3.5-K data were normalized to the level of the 295-K transmittance spectra at $500 \, \mu\text{m}$ ($20 \, \text{cm}^{-1}$) where the temperature dependence is small. The transmittance scale of the room temperature spectra is better than 1 per cent and the uncertainty in the normalization of the 3.5 K-data is $\sim \pm 10$ per cent. The data were then converted to absorbance units $[A = -\ln(\text{Transmittance})]$. Ripples in the spectra at wavelengths $\gtrsim 50 \, \mu\text{m}$ are an artefact of imperfections in the

thickness and the orientation of the samples and references relative to the beam.

Data were obtained for thick films of forsterite and olivine and for thinner films of olivine, and the pyroxenes. In the thick films, bands shortwards of $45 \, \mu\text{m}$ were frequently saturated (these bands were excluded from the figures and the analysis). The olivine and enstatite thin films were too thin for bands longwards of $45 \, \mu\text{m}$ to be resolved. The Bramble enstatite and diopside films were of sufficient thickness for the majority of bands to be seen at both temperatures. As the mass and grain size distribution of the silicate powder are unmeasured, the derived absorbances do not indicate mass density and the absorbance per unit area per unit mass cannot be estimated from these data at present.

4.3   Astronomical data

For comparison of our laboratory data with SWS and LWS spectra from *ISO*, we present observations of CPD $-56°8032$, a planetary nebula, the *ISO* spectrum of which was published by Cohen et al. (1999). We have reduced SWS observation 13602083 and LWS observation 08401538 and subtracted a polynomial continuum fit (with no physical significance) to show up the fine structure. Cohen et al. obtained a qualitative match to their spectrum with room-temperature forsterite (Mg_2SiO_4), orthopyroxene and clinopyroxene, using laboratory data by Koike, Shibai & Tuchiyama (1993) multiplied by 65 K (forsterite, clinopyroxene) and 90 K (orthopyroxene) blackbody continua. Features at 43 and $62 \, \mu\text{m}$ were matched with crystalline water ice. The wavelengths and FWHMs of the silicate peaks in their fits are marked (in Figs 4 and 5, later) by horizontal bars and vertical ticks. (It is beyond the scope of this paper to deduce the mineralogy of this source using our new laboratory data.)

5   RESULTS
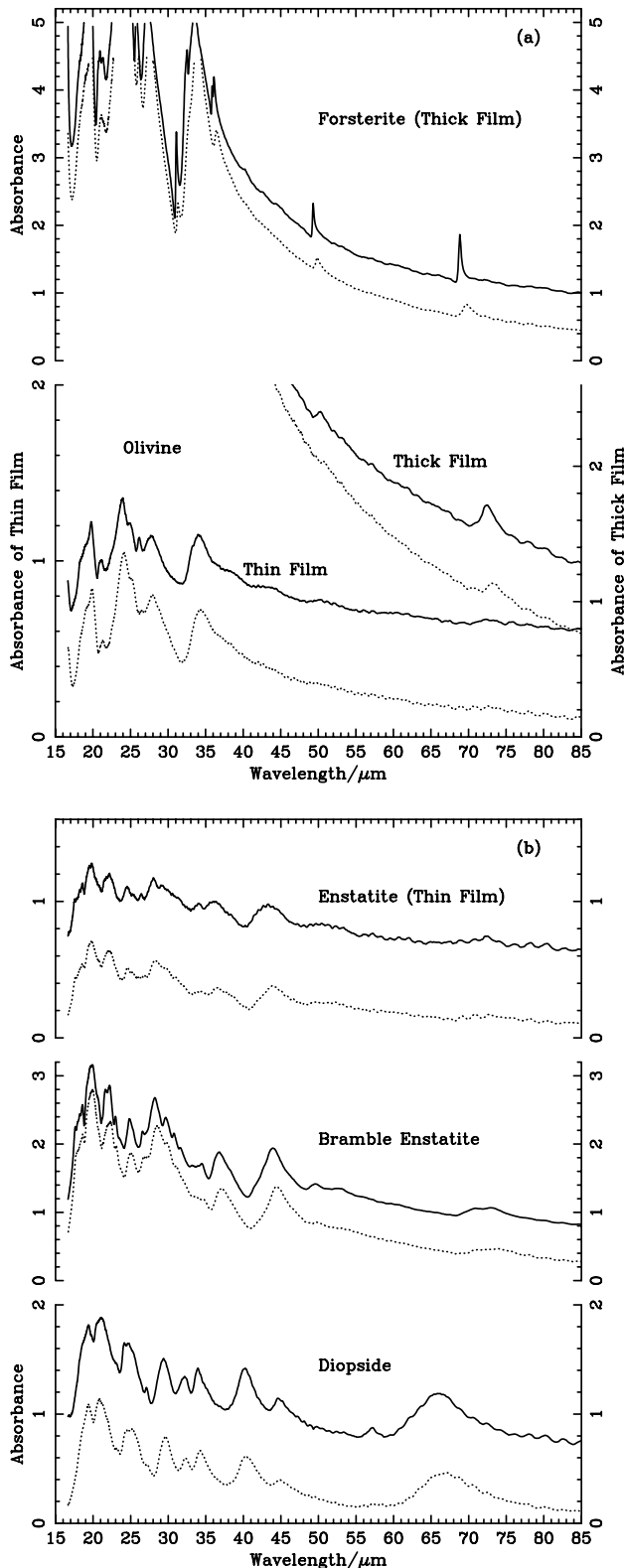
5.1   Overview of the laboratory data set

The 15–85 μm absorbance spectra of the olivines (forsterite and olivine), orthopyroxenes (enstatite and Bramble enstatite) and a clinopyroxene (diopside) are presented in Fig. 3. As it may be possible to estimate the grain size distribution and column density by electron microscopy at a later date, we present the measured values of absorbance for these samples.[1]

In general, (i) the room-temperature spectra look like low-resolution versions of their 3.5-K counterparts, even though the same spectral resolution was used for all these measurements; (ii) the relative absorbance of neighbouring peaks changes as the temperature is reduced; (iii) the wavelength of a peak decreases with temperature and the magnitude of the shift increases with the wavelength of the band. The effect of temperature is most noticeable in the forsterite spectra, with the bands becoming particularly narrow and strong: this difference with degree of ionic substitution is real because this is the only mineral devoid of Fe^{2+} or other cations substituting for Mg^{2+} in the crystal structure.

5.2   Effect of sample thickness

Comparison of the spectra of the 'thick' and 'thin' olivine films

---

[1]This normalization differs from that presented previously: Bowey et al. (2000) renormalized pairs of 3.5- and 295-K absorbance spectra to the absorbance of the highest room-temperature peak.

reveals that thick samples (i.e. larger amounts of powder embedded in the petroleum jelly) are required to see the comparatively weak 50- and 70-μm bands, and this has resulted in the saturation of the most prominent features of forsterite and thick olivine at wavelengths <40 μm. Hence, saturated features have been excluded from the presented data sets. The room-temperature spectra of the thin enstatite and thin olivine films contain no distinguishable features longwards of 45 μm. The Bramble enstatite and diopside films are of intermediate thickness, because bands are not saturated and the far-infrared peaks are clearly distinguishable from the underlying ripple.

5.3   Band splitting, band enhancements and changes in bandwidth

The detailed structure in the 18–38 and 38–80 μm regions are shown in Figs 4 and 5, respectively. Band splittings are seen shortwards of 38 μm, whilst wavelength shifts, band enhancements and changes in the FWHM of peaks are seen throughout the 18–80 μm range.

5.3.1   Band splitting

In both olivines the degenerate ~21-μm Mg^{2+} translation and SiO_4^{2-} rotation splits into two bands when cooled to 3.5 K (Fig. 4). The ~34-μm peak in forsterite is saturated, however this Mg^{2+} translation band is split in the 3.5-K olivine spectrum and the 36.45-μm 295-K Mg^{2+} translation peak in forsterite is also split at 3.5 K. The band splittings in forsterite are consistent with the peaks produced from different polarizations occurring at the same frequency (Hofmeister 1997); at 295 K this is an unresolved doublet. In the ortho-pyroxenes the band splitting is seen only in the three bands shortward of 23 μm. As the band assignments are undetermined in the enstatites, the cause of the splitting is unknown. In the diopside clinopyroxene only the degenerate Si–O–Si deformation at 20.91 μm is split.
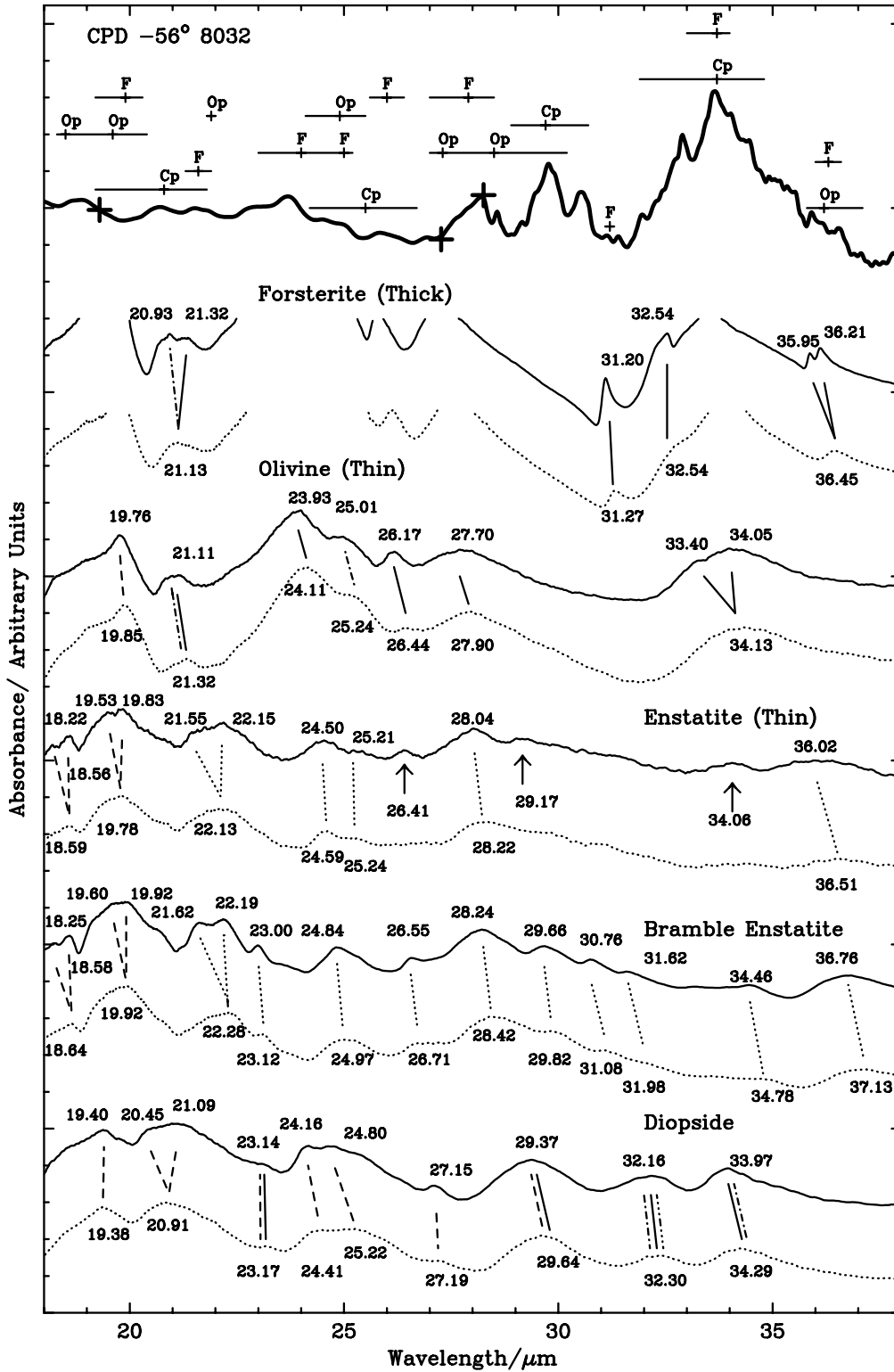
5.3.2   Band enhancements

The bands that are most strongly enhanced at low temperature, but which occur in both the room-temperature and the 3.5-K spectra, are the unsaturated forsterite peaks, the 25.44- (295-K) to 26.17-μm (3.5-K) olivine band, the 22.12- (295-K) to 23.00-μm (3.5-K) band of Bramble enstatite and the 25.22- (295-K) to 24.80-μm (3.5-K) band of diopside.

Some peaks that do not result from obvious splitting (or changes in the substrate) are seen only in the 3.5-K spectra. Such features occur in the 3.5-K thin enstatite spectrum at 26.41, 29.17 and 34.06 μm. As similar bands are seen in Bramble enstatite spectra obtained at both temperatures, we suggest that these features are enhanced at 3.5 K. Other peaks are seen in Bramble enstatite but not in enstatite (e.g. the 295-K 22.12-, 31.98- and 31.08-μm bands); this is probably a result of the greater thickness of the Bramble sample and to differences in the metal content in the two minerals. Extra bands are seen in the 3.5-K spectrum of Bramble enstatite at 53.91 μm, and in diopside at 57.16 μm.

5.3.3   Changes in bandwidth

Estimates of the FWHM of peaks that are well-separated from

Figure 3. Overview of data: 15- to 85-μm absorbance spectra of (a) olivines and (b) orthopyroxenes (enstatite and Bramble enstatite) and a clinopyroxene (diopside) at 295 K (dotted) and 3.5 K (solid). Each 3.5-K spectrum is displaced by 0.5 units above the 295-K spectrum of the same sample. For *thick films*, bands shortwards of 45 μm were saturated; for *thin films*, bands longwards of 45 μm were too weak to be resolved; the Bramble enstatite and diopside films were of intermediate thickness so that most bands were resolved at both temperatures.

Figure 4. Detailed structure in the 18–38µm wavelength range for the 295-K (*dotted*) and 3.5-K (*solid*) absorbance measurements, with the *ISO* spectrum of CPD −56°8032 (*thick solid line*) plotted for comparison. *ISO* observation: *bold crosses* indicate limits of spectral segments; horizontal bars with ticks indicate the FWHM and λ_{pk} (respectively) of the features in the Cohen et al. (1999) model obtained using room temperature data: 'F' = forsterite, 'Op' = orthopyroxene, 'Cp' = clinopyroxene). Laboratory spectra: lines and pairs of lines linking pairs of spectra respectively denote band shifts and band splitting. The styles of these lines indicate band assignments: *solid*, translation of Mg^{2+} and/or Fe^{2+} cations; *dashed*, deformation of Si−O−Si bands; *dot– dashed*, rotation of SiO_4^{4-} tetrahedra; *dash−dot-dot-dot*, translation of the silicate chain; *dotted*, the assignments of these bands are unknown; arrows denote bands seen only at 3.5 K. Offsets in the y-axis are arbitrary; pairs of spectra are normalized to the same level; hence the relative changes in band strength are real for individual samples.
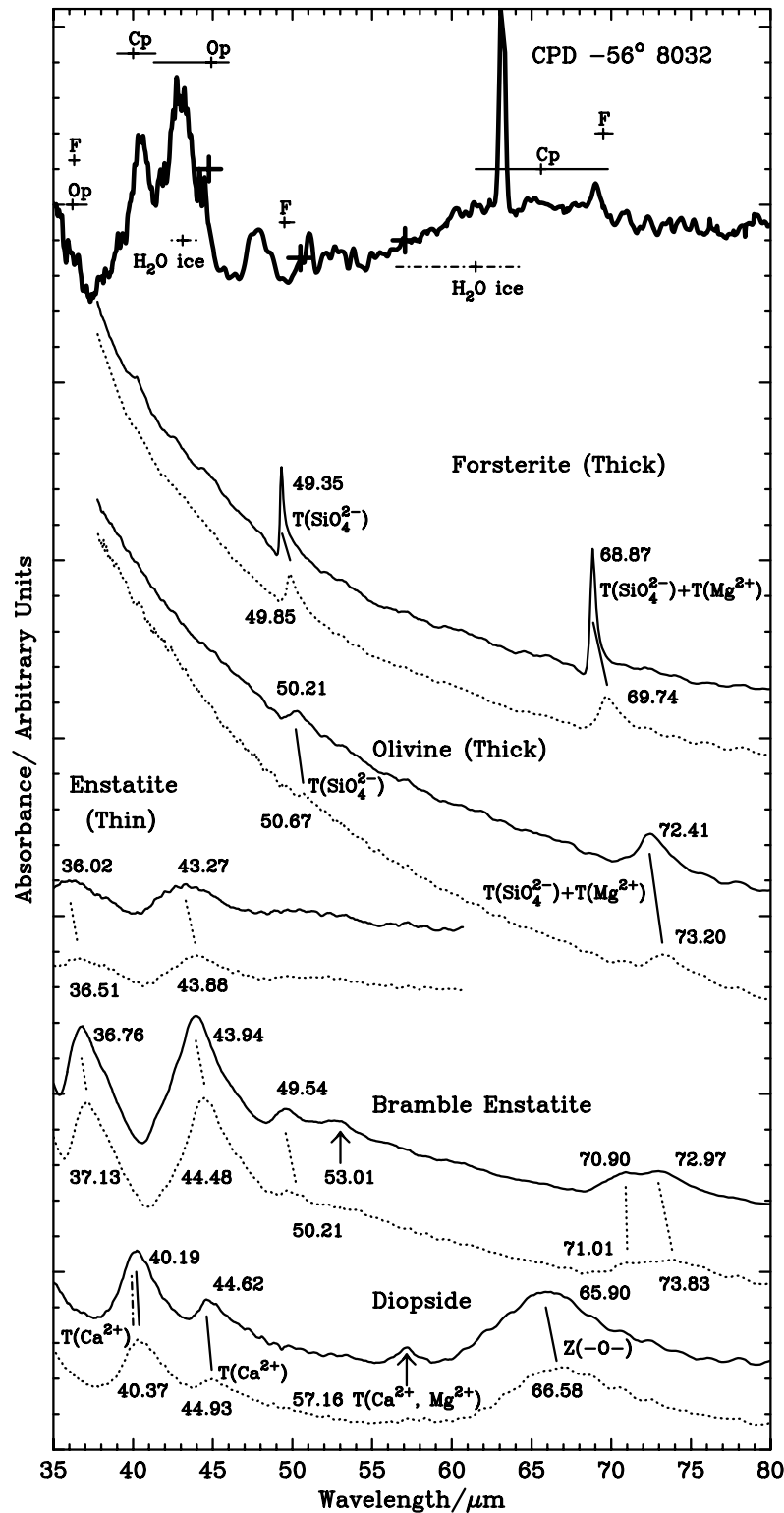
Figure 5. Band enhancements in the 38–80µm wavelength range compared with *ISO* data for CPD −56°8032. The *solid* lines linking the laboratory curves indicate band shifts due to ionic translations, T(ion), except Z(−O−) which is a zig-zag motion of the bridging oxygen atoms between silicate tetrahedra; *dot–dashed* lines indicate rotations of SiO_4^{2-} tetrahedra, band assignments for *dotted* lines are unknown. Arrows indicate extra bands observed at 3.5 K. See Fig. 4 for key to remaining symbols.

adjacent peaks and well-resolved are given in Table 2; peaks that are unresolved doublets at 295 K or are blended with stronger peaks have not been measured. The widths of isolated singlet peaks provide insight into the population of the vibrational modes.

FWHM values were extracted with the IDL GAUSSFIT routine, which approximates the continuum local to the peak with a quadratic equation and fits a Gaussian to the peak. As described in Section 3.2, singlet peaks in the 3.5-K spectra are narrower than
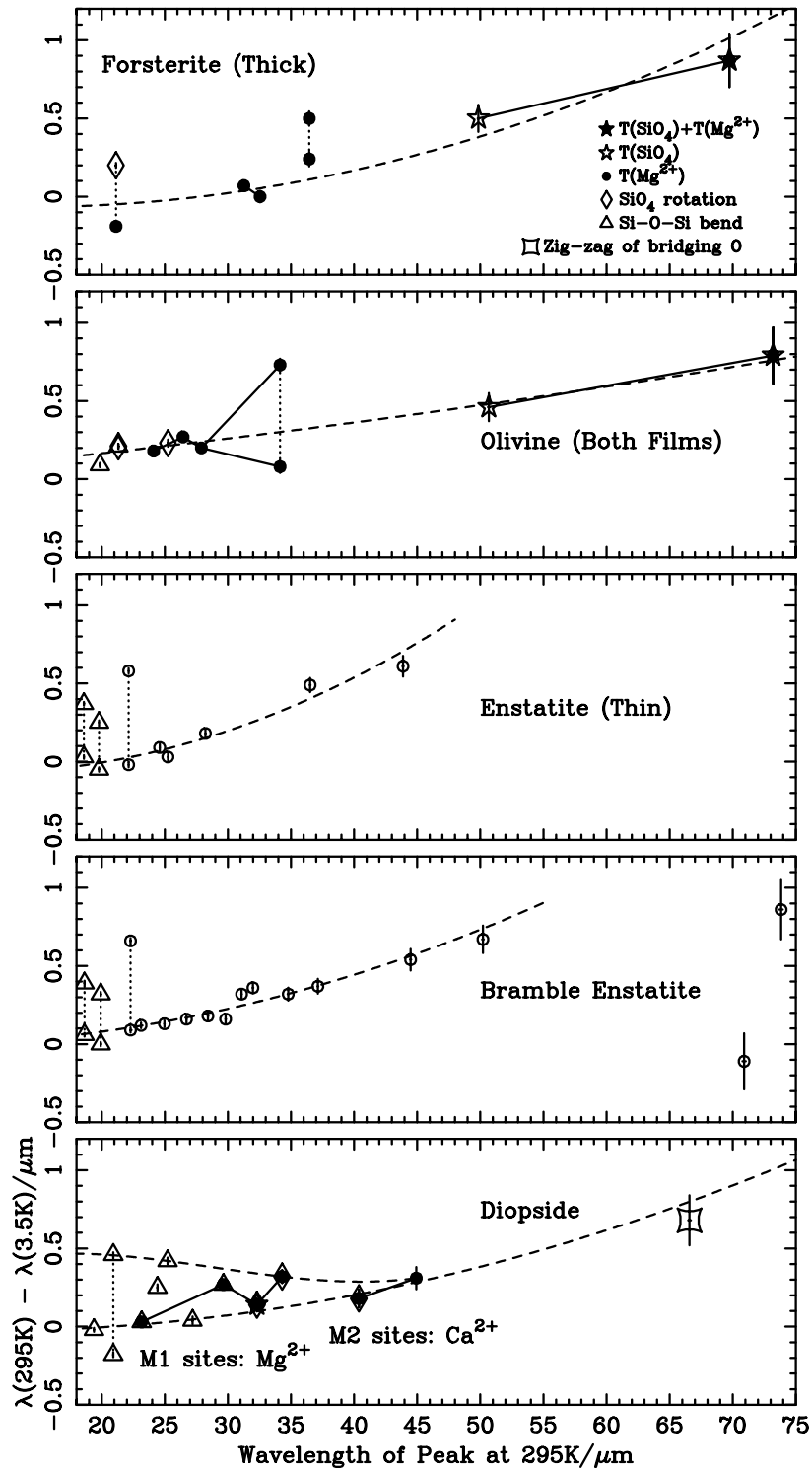
Figure 6. Shifts in the wavelengths of the peaks [λ(295 K)–λ(3.5 K)] versus the wavelength of the peaks at 295 K [λ(295 K)]. Error bars are plotted where they are larger than the plotting symbols; empty *circles* indicate unknown band assignments; *dotted* lines indicate degenerate 295-K bands which split at 3.5 K; *solid* lines connect bands that are produced by similar lattice components; *dashed* lines indicate fits obtained in Section 6.1.1. Some bands are missing from the forsterite and enstatite spectra because the samples were either too thick or too thin for them to be resolved.

those measured at 295 K. With the exception of the forsterite peaks, bandwidths in the 3.5 K spectra are ∼90 per cent of their 295-K widths, irrespective of the wavelength of the peak. The 31-, 49- and 69-µm bands of 3.5-K forsterite are, respectively, 90, 45 and 31 per cent of their 295-K widths; these bands arise from phonons along one direction within the lattice.

5.4 Wavelength shift and splitting patterns

In Fig. 6, the shifts in the peak wavelength of the bands between 295 and 3.5 K, λλ(295–3.5 K), are plotted as a function of the wavelength of the respective 295-K peaks. In general, bands shift to shorter wavelengths at 3.5 K and the magnitude

Table 2. Peak wavelengths (λ_{pk}) and FWHMs ($\Delta\lambda$) of selected bands.

Sample	λ_{pk} (295 K) μm	$\Delta\lambda$ (295 K) μm	λ_{pk} (3.5 K) μm	$\Delta\lambda$ (3.5 K) μm
Forsterite	31.27 ± 0.02	0.29 ± 0.02	31.20 ± 0.02	0.26 ± 0.02
	49.85 ± 0.06	0.56 ± 0.08	49.35 ± 0.06	0.25 ± 0.08
	69.74 ± 0.12	1.3 ± 0.1	68.87 ± 0.12	0.4 ± 0.1
Olivine	50.67 ± 0.06	–	50.21 ± 0.06	1.4 ± 0.1
	73.20 ± 0.13	1.8 ± 0.1	72.41 ± 0.13	1.6 ± 0.1
Bramble Enstatite	44.48 ± 0.05	2.76 ± 0.05	43.94 ± 0.05	2.49 ± 0.05
Diopside	40.37 ± 0.04	2.59 ± 0.05	40.19 ± 0.04	2.24 ± 0.05
	44.93 ± 0.05	1.77 ± 0.05	44.62 ± 0.05	1.63 ± 0.05
	66.58 ± 0.11	8.1 ± 0.2	65.90 ± 0.11	6.9 ± 0.2

The uncertainties in $\Delta\lambda$ are pessimistic and include the effects of spectral resolution, fringing and base-line estimates.

Table 3. Fits to $Rx = \lambda(295\,K)–\lambda(3.5\,K)$ using polynomial fits of the form $R = a + bx + cx^2$, where $x = \lambda_{pk}(295\,K)$, for the wavelength shift data plotted in Fig. 6.

| Mineral	Range μm	a $\times 10^{-3}$	b $\times 10^{-3}$	c $\times 10^{-3}$
Forsterite	31–70	−9.66	0.347	–
Olivine	24–74	7.47	0.0396	–
Enstatite	24–44	−14.0	0.686	–
Bramble Enstatite	23–52	−3.13	0.356	–
Diopside L^a	19–67	−5.44	0.262	–
U^b	25–45	62.4	−2.55	0.0294

^{a} Lower boundary of wavelength shifts: fit to 295-K peaks at 19.38, 23.17, 27.19, 32.30 μm and all peaks where $\lambda > 40$ μm.
^{b} Upper boundary of wavelength shifts: fit to 295-K peaks at 25.22, 34.29, 44.93 μm.

of the band shift increases with increasing wavelength, from ~0–0.2 μm at 25 μm to ~0.9 μm at 80 μm. However, the shift patterns are quite complicated because different peaks have different origins in the lattice. The situation is complicated in some of these spectra, because we have not been able to resolve all the peaks in the thick forsterite and thin enstatite. Measurements of the spectra of other film thicknesses are required to determine the low-temperature behaviour of all the infrared peaks.

The shift patterns and band splittings are similar within a solid solution series if the lattice structure is the same. For example, the ~50-μm and ~70-μm bands exhibited by forsterite and olivine shift by similar amounts, −0.5 μm and −0.9 μm, respectively, when the minerals are cooled from 295 to 3.5 K. The increase in the energies of these SiO_4^{4-} and combined SiO_4^{4-} and Mg^{2+} translations at 3.5 K indicates a contraction of the lattice as the temperature is reduced; sharpening of the bands is caused by a reduction in phonon scattering at 3.5 K.

The ortho- and clinopyroxenes exhibit different shift and splitting patterns. The band shifts in Bramble enstatite and in enstatite increase fairly uniformly with wavelength. However, shifts between neighbouring bands in diopside clinopyroxene vary by up to 0.3 μm and between 27 and 41 μm the pattern is almost saw-tooth. The complex shift pattern of diopside is probably caused by the difference in the size and mass of the Ca^{2+} and Mg^{2+} cations which respectively occupy the M2 and M1 sites. Band splitting in the three 18–22.5 μm bands is common to both orthoenstatites: the Si−O−Si shifts in both
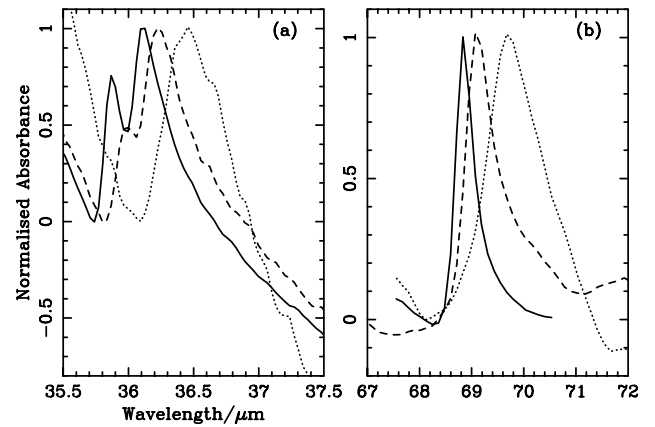
Figure 7. Comparison between 3.5 K (*solid*), 77 ± 5 K (*dashed*) and 295 K (*dotted*) forsterite spectra. 77-K spectra were obtained by placing the forsterite sample in a cold finger cooled by liquid nitrogen within the output beam of the spectrometer.

minerals are ~0.0 and −0.4 μm and the Mg^{2+} shifts of the ~22.5-μm peak are 0.0 and −0.5 μm. The splittings are caused by a reduction in the widths of the peaks, and by different orientations (polarizations) of the bonds within the lattice because the different crystallographic axes contract with temperature at different rates.

6   DISCUSSION

6.1   Astrophysical implications

These determinations of the relationship between temperature and band shifts and band splitting could help in reaching a better understanding of the mineralogy of astronomical regions showing optically thin silicate bands in the far infrared. Such temperature-dependent laboratory measurements could greatly benefit the elucidation of the physical properties of dusty environments.

6.1.1   Limits on the effect of temperature on λ_{pk}

The far-infrared bands observed in many astronomical environments are wavelength-shifted with respect to bands of similar shape observed in room-temperature laboratory spectra (Molster 2000). Wavelength shifts can be introduced by temperature differences, but they can also be introduced by other factors such as chemical and isotopic composition and degree of crystallinity. To place limits on the contribution of temperature to the wavelength shift of a peak in astronomical data, fits to the ratio, $R = [\lambda(295\,K)–\lambda(3.5\,K)]/\lambda(295\,K)$, for peaks that did not split at 3.5 K were obtained over the wavelength ranges specified in Table 3. Linear fits to R were obtained using the IDL LINFIT routine; the fit to the upper limit of the diopside shifts was obtained with the IDL POLYFITW routine. Polynomial fits to the wavelength shifts of singlet bands between 295 and 3.5 K are plotted in Fig. 6 and the coefficients of these fits are listed in Table 3.

6.1.2   Determination of grain temperatures

Our results indicate that suitable high-resolution spectra obtained at a range of cryogenic temperatures can be used to determine the characteristic temperatures of specific grain populations in astronomical spectra. An emission feature that peaks near 69 μm in circumstellar spectra has been identified with forsterite (Malfait,

Waelkens & Vandenbussche 1998). However, the astronomical feature is shifted relative to room-temperature laboratory data, which give $\lambda_{pk} = 69.74\,\mu m$ (Fig. 5 and Table 2). In Fig. 7(b) we compare the shape of the 69-μm band of our laboratory forsterite spectra obtained at three different temperatures. The spectral resolution of the *ISO* LWS grating spectrometer at this wavelength was 0.3 μm, compared with the laboratory feature's FWHM of 1.3 μm at 295 K and 0.4 μm at 3.5 K, while the LWS wavelength precision was 0.03 μm, compared with the shift of 0.9 μm in the peak wavelength between 295 and 3.5 K. Therefore the derivation of characteristic grain temperatures from *ISO* spectra is quite feasible (see also Molster 2000) and will be reported on in a subsequent paper (Bowey et al., in preparation). Band splitting and band shifts at other wavelengths, for example the splitting in the 36.5-μm forsterite band shown in Fig. 7(a), could also be used to determine grain temperatures if the spectral resolution and signal-to-noise ratio of the astronomical data were sufficiently high. The relation between the derived characteristic grain temperatures at different wavelengths may aid the determination of the spatial distribution of the dust.

6.1.3 Effect on inferred mineralogical compositions and dust masses

The absorption coefficients of the forsterite bands are enhanced at 3.5 K compared with room-temperature values. In contrast, there is little change in the absorption coefficients of most of the pyroxene features. Therefore, the true mass ratio of forsterite to enstatite could be smaller than estimated using room-temperature laboratory data. More mass is required to reproduce the strengths of many features in *ISO* spectra using room-temperature optical constants than would be required at the likely temperatures of the astronomical grains. Measurements of the temperature dependence of the mass absorption coefficients are required in order to obtain the true relative mineralogical composition and dust masses.

7 SUMMARY

We have obtained $0.25\,cm^{-1}$ resolution 15–85 μm spectra of powdered minerals embedded in petroleum jelly at $295 \pm 2\,K$ and $3.5 \pm 0.5\,K$. The samples were two olivines, forsterite (Mg_2SiO_4) and olivine var. peridot $Mg_{1.77}Fe_{0.20}Al_{0.01}Ni_{0.01}SiO_4$, two orthoenstatites, enstatite and Bramble enstatite, and a clinopyroxene (MgCa diopside).

The following general conclusions can be drawn.

(i) The room temperature spectra look like lower resolution versions of their 3.5-K counterparts. In both of the olivines the degenerate ~21-μm Mg^{2+} translation and SiO_4^{2-} rotation splits into two bands when cooled to 3.5 K. The ~34-μm peak in forsterite is saturated, however this Mg^{2+} translation band is split in the 3.5-K olivine spectrum and the 36.45-μm 295-K Mg^{2+} translation peak in forsterite is also split at 3.5 K. In the orthoenstatites, band splitting is seen only in the three bands shortward of 23 μm. In the MgCa diopside clinopyroxene only the 20.91-μm degenerate $Si-O-Si$ deformation is split. Different sample thicknesses must be measured to verify that no splitting is seen in other bands.

(ii) The wavelength of a peak decreases with temperature and the magnitude of the shift increases with the wavelength of the band, from ~0–0.2 μm at 25 μm to ~0.9 μm at 80 μm. However, the shift patterns are quite complicated and depend on lattice structure

as well as stoichiometry, because they differ between ortho- and clino-pyroxenes. For example, the band shifts in Bramble enstatite and enstatite increase with wavelength. However, in the diopside clinopyroxene the shifts between neighbouring bands vary by up to 0.3 μm – between 27 and 41 μm the pattern is almost saw-tooth. The situation is complicated in these spectra because we have not been able to resolve all the peaks at all temperatures. For the olivines and enstatites the wavelength shifts of bands that are singlets at 295 and 3.5 K can be approximated by polynomials of the form $ax + bx^2$ where $x = \lambda_{pk}(295\,K)$ and coefficients a and b differ between minerals. Lower limits to the wavelength shifts for diopside can be obtained using polynomials of this form, however a third-order term is required to obtain the upper estimates for wavelength shifts in the 20–41 μm region.

(iii) Bands sharpen as the temperature is reduced. At 3.5 K the widths of isolated single bands in the olivine, enstatites and diopside are ~90 per cent of their 295-K widths. However, in forsterite, the 3.5-K, 31-, 49- and 69-μm bandwidths are, respectively, 90, 45 and 31 per cent of their 295-K widths.

(iv) The relative absorbances of neighbouring peaks change and bands sharpen as the temperature is reduced; this effect is most noticeable in the forsterite spectra. Peaks at 53.91 μm in Bramble enstatite and at 57.16 μm in diopside appear only in the 3.5-K spectra.

Our results show that comparison between the band shifts, bandwidths and band splitting in laboratory data obtained at a range of temperatures with astronomical far-infrared spectra can allow a determination of the characteristic temperatures of crystalline grains responsible for the optically thin emission features. Further low-temperature spectra at a range of temperatures are required to ascertain the precise temperature dependence of the shift, because the relationship between T and λ_{pk} is unlikely to be linear between 295 and 3.5 K and it is possible that the bands stop shifting at some temperature above 3.5 K. Ultimately it may be possible to determine the temperature of distinct grain populations by comparison of the observed peak wavelengths and FWHMs with laboratory spectra. As the absorption coefficients of bands in laboratory spectra also vary with temperature, new measurements may allow better estimations of grain masses and silicate mineralogy. Additional high-resolution laboratory spectra of a larger variety of silicates, at a larger number of temperatures, are desirable for comparison with *ISO* data and with future measurements obtained by spectrometers on board SIRTF, Herschel and the NGST. These laboratory measurements are planned.

REFERENCES

Agladze N. I., Sievers A. J., Jones S. A., Burlitch J. M., Beckwith S. V. W., 1996, ApJ, 462, 1026

Bowey J. E., Lee C., Hofmeister A. N., Tucker C., Ade P. A. R., 2000, ESA Special Publication SP-456, p. 399

Cohen M., Barlow M. J., Sylvester R. J., Liu X. W., Cox P., Lim T., Schmitt B., Speck A. K., 1999, ApJ, 513, L135

Crovisier J. et al., 2000, in Sitko M. L., Sprague A. L., Lynch D. K., eds, ASP Conf. Ser. Vol. 196, Thermal Emission Spectroscopy and Analysis of Dust, Disks, and Regoliths. Astron. Soc. Pac., San Francisco, p. 10

Day K. L., 1976, ApJ, 203, L99

Ferraro J. R., 1984, Vibrational spectroscopy at high external pressures: the diamond anvil cell. Academic Press, New York, p. 264

Henning Th., Mutschke H., 1997, A&A, 327, 743

Hofmeister A. M., 1997, Phys. Chem. Miner., 24, 535

Hofmeister A. M., 1999, Sci, 283, 1699

Hofmeister A. M., Mao H. K., 2001, Am. Miner., 86, 622

Jasperse J. R., Kahan A., Plendl J. N., Mitra S. S., 1964, Phys. Rev., 146, 526542

Joblin C., Boissel P., Léger A., D'Hendecourt L., Défourneau D., 1995, A&A, 299, 835

Kachare A., Andermann G., Brantley L. R., 1972, J. Phys. Chem. Solids, 33, 467

Koike C., Shibai H., Tuchiyama A., 1993, MNRAS, 264, 654

Malfait K., Waelkens C., Vandenbussche B., 1998, Ap&SS, 255, 43

Malfait K., Waelkens C., Bouwman J., De Koter A., Waters L. B. F. M., 1999, A&A, 345, 181

Mennella V., Brucato J. R., Colangeli L., Palumbo P., Rotundi A., Bussoletti E., 1998, ApJ, 496, 1058

Molster F. J., 2000, PhD thesis, Univ. Amsterdam

Sylvester R. J., Kemper F., Barlow M. J., de Jong T., Waters L. B. F. M., Tielens A. G. G. M., Omont A., 1999, A&A, 352, 587

Tomisaka T., Iishi K., 1980, Mineralogical Journal, 10, 81

Waters L. B. F. M. et al., 1996, A&A, 315, L361

Wooten F., 1972, Optical properties of solids. Academic Press, San Diego, p. 46

This paper has been typeset from a TEX/LATEX file prepared by the author.